

Effect of Damp-Heat Aging on the Structures and Properties of Ethylene-vinyl Acetate Copolymers with Different Vinyl Acetate Contents

Xu-Ming Shi, Jun Zhang, Deng-Ru Li, Shuang-Jun Chen

Department of Polymer Science and Engineering, College of Materials Science and Engineering, Nanjing University of Technology, Nanjing 210009, People's Republic of China

Received 19 December 2007; accepted 6 November 2008

DOI 10.1002/app.29659

Published online 17 February 2009 in Wiley InterScience (www.interscience.wiley.com).

ABSTRACT: We reported herein the damp-heat aging of ethylene-vinyl acetate copolymers (EVA) with different vinyl acetate (VAc) contents simultaneously for weeks. The aging was carried out under temperature of 40°C and relative humidity of 93% in air atmosphere. The changes of copolymers' structures and properties were investigated by means of FTIR, wide angle X-ray diffraction (WAXD) and differential scanning calorimetry (DSC) and mechanical tests. CI values derived from ATR-FTIR spectra have a decrease when aging time is 1 week and then increase during damp-heat aging process which suggests the first loss then incorporation of O=C

group. WAXD infer that the narrowing trend of FWHM and increase of crystal sizes may attribute to the melting and re-crystallization of secondary crystallization, which is also confirmed by DSC results. Mechanical tests including Shore A and Shore D hardness, modulus at 100%, tensile strength and elongation at break, are all depending on the primary crystallization and influenced little by damp-heat aging. © 2009 Wiley Periodicals, Inc. *J Appl Polym Sci* 112: 2358–2365, 2009

Key words: damp-heat aging; structure; crystallization; mechanical properties

INTRODUCTION

Because of restricted properties and limited use of homopolymers alone, copolymers were explored to widen the utilization of these polymers in different industries.¹ Ethylene-vinyl acetate (EVA) copolymers have been widely used for many years because the materials were available commercially in the middle of the 20th century. Versatile materials such as films, coatings, foams, cables, hot-melt adhesives, and other commonly used products can be made of EVA copolymers either original or blended with other materials. The copolymers were often produced by continuous bulk polymerization under high pressure.² Their properties were easily variable by the adjustment of the comonomer ratio. When the VAc content was low, the copolymers are more akin to polyethylenes and have enough ability to crystallize, but for high VAc content the pendent acetoxyl is excessive enough and prevents adjacent polyethylene chains packing into the crystal lattice,³ then totally amorphous and rubber-like EVA is expected when the VAc content is more than 43% by weight as indi-

cated by Kamath et al.⁴ However, during long-term use, the EVA copolymers have to undergo aging or degradation like other polymer materials due to the combined actions of sunlight, heat, moisture, atmospheric oxygen and so on. To solve this problem, essential attentions should be drawn on their different degradation behaviors and mechanisms.

Up to now, many studies have focused on either thermal degradation^{5–12} or photodegradation.^{13–18} Despite those significant researches covering thermal aging or photothermal aging of EVA copolymers, it seems there is scarcely study on the damp-heat aging of EVA copolymers, which is conducted under relatively low temperature and high relative humidity. If EVA products such as soles, coatings or even cable insulator are put to use, they are often subject to moisture and the materials will undergo substantial damp aging that might have decisive effect on the properties.

In this experiment, EVA copolymers with different VAc contents were exposed in a damp-heat environment with low temperature and high relative humidity for total 8 weeks. The three copolymers remained to be solid materials as they are usually like in practical use condition. Changes in their structure and properties during damp-heat aging were investigated by infrared spectroscopy (IR), wide angle X-ray diffraction (WAXD), differential scanning calorimetry (DSC) and mechanical test.

Correspondence to: J. Zhang (zhangjun@njut.edu.cn).

EXPERIMENTAL

Materials

Three commercial EVA copolymers with different VAc contents were used for investigation. EVA14 (VAc content 14 wt %) and EVA18 (VAc content 18 wt %) were produced by Beijing Organic Chemical Plant, China; whereas EVA28 (VAc content 28 wt %) was produced by Sumitomo Chemical (Japan). They were all supplied in granular forms.

Samples preparation

The EVA copolymers were received as pellets and first injected by small plunger injection molding machine of RR/TSMP type made in United Kingdom by RAY-RAN (POLYTEST) Test Equipment. The barrel temperature was set as 170°C for EVA28 and 190°C for EVA14 and EVA18, whereas the mold temperature was set as 30°C with maximum injection pressure of 0.76 MPa (110 psi). The mould has a rectangular rut and the depth was about 2 mm. After laminated, the sheets were cut into dumbbell pieces for tensile testing or retain for infrared spectrometer analysis. In addition, thin films about 0.3 mm of these EVA copolymers for measurements of DSC and WAXD were prepared from the injected sheets, which were pressed under 5 MPa between two metal platens at the same temperature of 120°C and cooled between another two metal platens under room temperature.

Damp-heat aging

Sheet and film samples of EVA prepared above were both placed in a damp-heat testing environment with air blowing for aging testing at different intervals of time up to 8 weeks, where the relative humidity (RH) was 93₋₃⁺²% and the temperature was (40 ± 2)°C. All the conditions in the damp-heat aging refer to GB/T12000–2003 established in China. As 40°C is lower than the softening points of these kinds of EVA, these copolymers were solid like rather than melting or transforming during the aging.

Fourier transform infrared spectroscopy analysis

FTIR spectra were obtained by Attenuated Total Reflectivity (ATR) technique to monitor the changes in structure of the three copolymers during damp-heat aging. The instrument used here was IFS 66/S produced by BRUKER Company in Germany. And the scanning range was 4000~580 cm⁻¹ with resolution of 4 cm⁻¹ at 32 scans. To eliminate the difference of physical contact between sample and reflection element every time and gain a quantitative measure of the absorbance peak intensity of the

functional group, carbonyl index (CI) was introduced here and it was determined using the following expression^{19–21}:

$$CI = \frac{A_{1735}}{A_{720}}$$

where A_{1735} is the absorbance of ester (acetate) carbonyl stretching vibration at 1735 cm⁻¹ and A_{720} is the absorbance of the CH₂ in-plane deformation rocking at 720 cm⁻¹; the latter absorption is an internal standard to compensate the signal differences due to surface factor.

Wide angle X-ray diffraction

WAXD measurements of different EVA copolymers before and after aging were carried out on an XRD-6000 diffractometer produced by Shimadzu (Japan). The diffraction data were collected from 5 to 45° with a scanning rate of 4°/min at an operating voltage of 40 kV and a current of 30 mA using Cu K α_1 (1.541 Å) radiation. Using FWHM (full width of diffraction angle at half maximum diffraction intensity) of XRD peak, an approximate average crystal size, D which is the thickness of the crystal perpendicular to the lattice planes can be estimated from Scherrer's equation²²:

$$D = \frac{K\lambda}{\beta \cos \theta}$$

Where, K is a constant that is close to 0.89, β is the FWHM in radian, λ and θ are the wavelength of X-ray and the diffraction angle, respectively.

Differential scanning calorimetry

The melting behaviors of EVA copolymers after aging were evaluated using Pyris1 type of DSC instrument produced by Perkin Elmer. Samples weighting about 12 mg were tested with a heating rate of 10°C/min, and Argon purge gas with a flux of 20 mL/min was used to prevent oxidative degradation of samples during the heating run. Here the scanning range was from 0°C to 150°C. The relative crystallinity (X_c) of the samples was calculated with the following expression:

$$X_c = \frac{\Delta H_f}{\Delta H_f^*} \times 100\%$$

Where ΔH_f^* is the enthalpy of fusion of the perfect polyethylene (PE) crystal and ΔH_f is the enthalpy of fusion of the EVA samples, respectively. The value of ΔH_f^* for PE is 277.1 J/g.²³

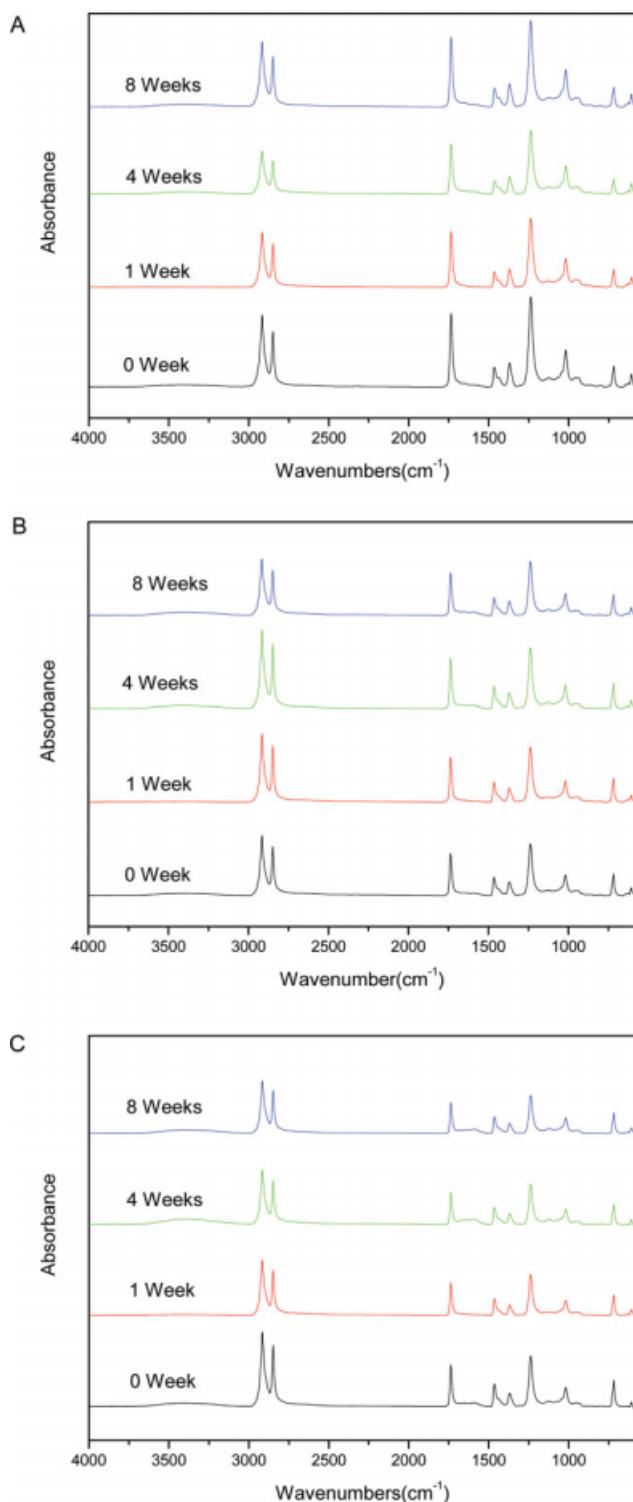


Figure 1 ATR-FTIR spectra of (A) EVA14; (B) EVA18; (C) EVA28 for different damp-heat aging time. [Color figure can be viewed in the online issue, which is available at www.interscience.wiley.com.]

Mechanical test

Shore A and Shore D hardness of original and damp-heat aged EVA specimens were recorded by durometers made in China, according to ISO 868

and ISO 7619, respectively. The tensile strength and elongation at break were measured by a MZ-2000C electronic pulling tester produced by Shenzhen Sans Test Machine (China), with a crosshead speed of 50 mm/min and a gauge length of 25 mm. The test was conducted under the condition according to ISO 527. Modulus at 100% was also considered here because the elongation at break was higher than 100%.

RESULTS AND DISCUSSION

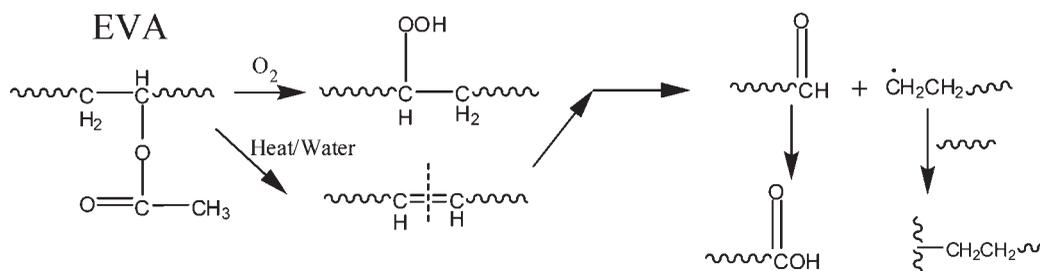
ATR-FTIR

To investigate the chemical structure changes after damp-heat aging of the three EVA copolymers, ATR-FTIR spectra were recorded on the surfaces of samples. Figure 1(A–C) describe the ATR infrared spectra of the three EVA copolymers with different VAc contents before and after damp-heat aging for 1 week, 4 weeks and 8 weeks, respectively. As shown in Figure 1, for ethylene segments, the characteristic absorption peaks are as follows: 2920 cm^{-1} and 2852 cm^{-1} attributed to the symmetrical and asymmetrical stretching vibration of methylene; 1465 cm^{-1} attributed to deformation vibration of methylene; 1370 cm^{-1} attributed to flexural vibration of methyl; 721 cm^{-1} attributed to inner rocking vibration of methylene. Characteristic absorption peaks of VAc groups are as follows: 1735 cm^{-1} attributed to stretching vibration of C=O band; 1237 cm^{-1} attributed to asymmetrical stretching vibration of C–O band; 1020 cm^{-1} attributed to symmetric stretching vibration of C–O–C band. As aging time increases from 1 to 8 weeks, thermo, oxidation and water all have effect on the degradation of the blends.

The course of damp-heat aging is followed by using a carbonyl index (CI) derived from ATR-FTIR measurements. Table I shows the changes of CI of EVA copolymers with different damp-heat aging time. Before aged, the CI increased regularly with

TABLE I
CI Data of the Three EVA Copolymers After Damp-Heat Aging from ATR-FTIR Spectra

Sample	Aging time (week)	CI value
EVA14	0	1.71
	1	1.53
	4	1.70
	8	1.61
EVA18	0	1.95
	1	1.88
	4	1.99
	8	2.06
EVA28	0	3.51
	1	3.12
	4	3.38
	8	3.55



Scheme 1 Damp-heat aging mechanism of EVA.

VAc content. As aging time increases, it can be observed that the CI values first have a little decrease from 0 week to 1 week for the three EVA. When the aging time increases further to 8 weeks, the CI values increase equal to or more than those of the original samples. The phenomenon depends on the damp-heat aging mechanism of EVA, as shown in Scheme 1. In the presence of thermo and water, EVA copolymers probably undergo a pyrolysis involving two-step decomposition: an acetate pyrolysis of the copolymer leaving a polyunsaturated linear hydrocarbon and evolving mainly acetic acid, followed by the breakdown of the hydrocarbon backbone to produce a large number of straight-chain hydrocarbon products for nonoxidative decomposition. However, in the presence of oxygen, degradation of EVA produces first the ketone formation via acetaldehyde formation, and then the formation and destruction of aldehydes to form carboxylic acids. That is to say, the main sequence of damp-heat aging on three EVA is the competition of loss or formation of O=C group, which can explain the aforementioned phenomenon that CI values of the EVA have first decrease and then increase during damp-heat aging process.

Crystallization behaviors

Crystallization of polyethylene from the melt state can be described generally by two stages: primary crystallization and secondary crystallization. During secondary crystallization, it is suggested that the dominant secondary crystallization process is by nucleation on preexisting crystals and these secondary crystals are confined to the amorphous regions surrounding the lamellar aggregates.²⁴ It has been observed that in spherulites the long-chain fractions are enriched in the early-grown thick crystals called dominant lamellae, whereas the short-chain fractions are rich in the later-grown thin crystals called subsidiary lamellae.²⁵ Under even larger supercoolings, co-crystallization of long-chain and short-chain fractions occurs without any segregation. The crystallization behavior of semi-crystalline EVA during

damp-heat aging is investigated by WAXD and DSC here.

WAXD

X-ray diffraction patterns for the EVA copolymers before and after aging for 1 week and 8 weeks are displayed in Figure 2. It is shown from Figure 2 that before aging all of the EVA copolymers have three perceptible diffractive peaks around 21.5°, 23.9°, and 36.3° relative to typical (110), (200), and (020) crystallographic planes of polyethylene respectively. The presence of these characteristic diffractive crystallographic planes clearly indicates all of the EVA copolymers have an orthorhombic unit cell structure originally.²⁶ However, the typical (001) crystallographic plane at 19.5° and (200) at 23.2° assigned to

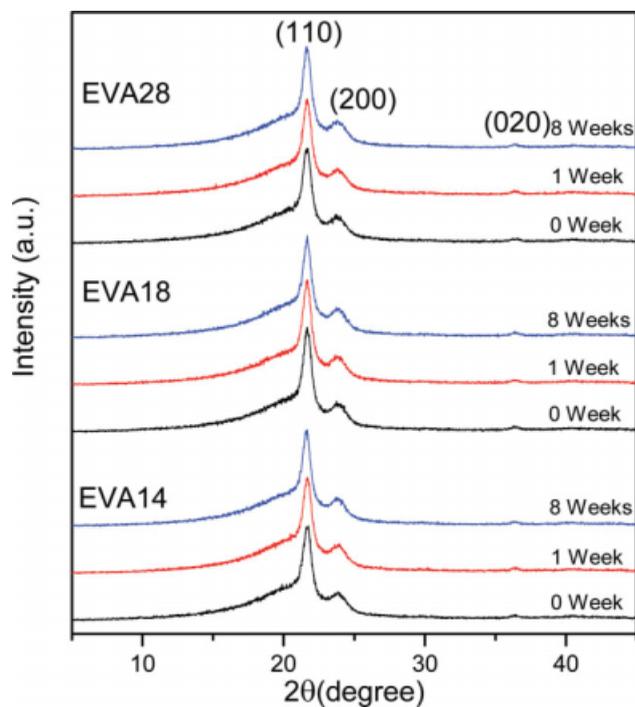


Figure 2 WAXD patterns of the three EVA copolymers before and after damp-heat aging for several weeks. [Color figure can be viewed in the online issue, which is available at www.interscience.wiley.com.]

TABLE II
WAXD Data of the Three EVA Copolymers After Damp-Heat Aging

Sample	Aging time (week)	2 θ (°)	<i>d</i> value (Å)	FWHM (°)	<i>D</i> ₁₁₀ (Å)
EVA14	0	21.5	4.14	0.87	92.3
	1	21.4	4.14	0.87	92.4
	8	21.5	4.14	0.85	93.9
EVA18	0	21.4	4.14	1.18	67.9
	1	21.4	4.15	1.06	75.6
	8	21.4	4.15	1.08	73.9
EVA28	0	21.1	4.21	1.92	41.6
	1	21.3	4.17	1.64	48.7
	8	21.4	4.17	1.50	53.2

monoclinic crystalline phase could not be observed obviously from these diffractive curves.²⁷ It is considered from the WAXD curves that no notable crystalline phase other than orthorhombic crystalline phase exists in these EVA copolymers before aging. It also can be inferred that the crystalline phase did not change significantly during the damp-heat aging.

To give some quantitative comparisons, diffractive parameters of the strongest diffraction peak corresponding to (110) crystallographic plane are listed in Table II.

Calculated by Scherrer's equation, crystal sizes of (110) plane increase to different extents for the three EVA copolymers with aging time. Before aging, EVA14 has the lowest VAc content and the crystal size of (110) is about 92.3 Å which is higher than 67.9 Å of EVA18 or 41.6 Å of EVA28. For EVA14, the crystal size of (110) increases a little to be 93.9 Å when aging time is 8 weeks. Especially, it almost increases by 30% after aging for 8 weeks in the case of EVA28. The different changes of the crystal size among the three EVA copolymers originate from their different VAc contents. Because of low VAc content, EVA14 should have the least completion of secondary crystallization among the three EVA polymers.²⁸

It is noticed secondly that the changes of FWHM occur after aging for 1 week or 8 weeks. Especially, the FWHM of EVA28, it narrowed from 1.92° to 1.64° after aging for 1 week, and after 8 weeks the FWHM have showed more than 20% decrease already. The narrowing trend of FWHM may also attributed to the melting and recrystallization of secondary crystallization.

DSC

For further study on the crystallization of the three EVA copolymers before and after damp-heat aging, some representative DSC thermograms are displayed

in Figure 3 and the corresponding results are given in Table III. In Figure 3, the peaks in the low and high melting temperature ranges are denoted as L-peak and H-peak. The H-peaks and L-peaks are attributed to the primary and secondary crystallization,^{29,30} respectively.

From Table III, it can be seen in detail that before aging the melting peak temperature of the H-peak decreases as the VAc content increase, and the same trend is observed for the L-peak. Such a result can be explained by the fact that the EVA copolymer with higher VAc content has shorter average ethylene sequence length and forms smaller or more defective crystals whose melting require relative lower temperature. It is further found that before aging as the VAc content increases from 14 to 28%, the peak temperature of the L-peak gets a decrease value of 11°C that is less than 20.1°C of the H-peak. The L-peak shifts to high temperature whereas the H-peak is still steady after damp-heat aging for 1 week or even 8 weeks indicating that the VAc content has more effect on the primary crystallization than the secondary crystallization relatively.

It is interesting to notice that after damp-heat aging for 8 weeks, the L-peaks of three EVA copolymers reach almost the same temperature around 58°C which is 18°C higher than the aging temperature. When EVA copolymer is aged under the temperature (it is 40°C in the damp-heat aging) upper its glass transition temperature, the secondary crystallization will continue and many crystals become bigger or more perfect and it can also be confirmed by the WAXD analysis. The similar result is also observed in the aging of ethylene- α -olefin copolymers.³¹

Table III also shows that before aging EVA14 has a melting range of 61.6°C which is wider than

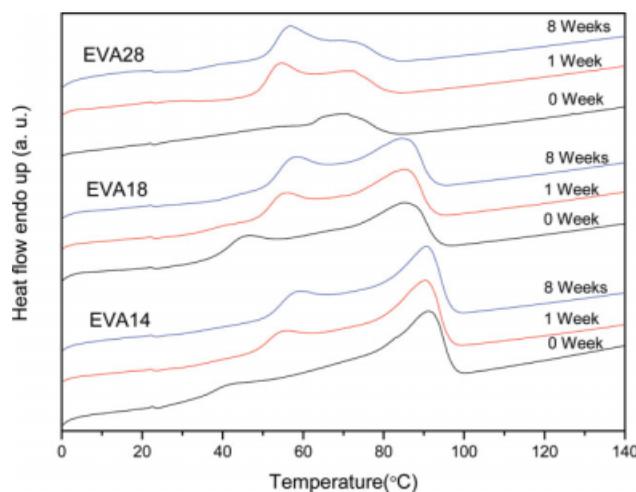


Figure 3 DSC curves of the three kinds of EVA copolymers before and after damp-heat aging for several weeks. [Color figure can be viewed in the online issue, which is available at www.interscience.wiley.com.]

TABLE III
DSC Melting Results of the Three EVA Copolymers After Damp-Heat Aging

Sample	Aging time (week)	T_m^{on} (°C)	T_m^{pl} (°C)	T_m^{ph} (°C)	T_m^{f} (°C)	ΔT_m (°C)	ΔH_m (J/g)	X_c (%)
EVA14	0	35.7	41.7	91.3	97.3	61.6	72.1	26.02
	1	46.1	54.9	90.3	96.2	50.1	74.5	26.88
	8	49.4	58.4	90.6	96.7	47.3	75.1	27.10
EVA18	0	37.8	45.5	85.2	93.6	55.8	64.3	23.20
	1	47.3	55.4	84.7	92.1	44.8	64.9	23.42
	8	49.2	57.6	84.4	92.1	42.9	65.8	23.75
EVA28	0	48.8	52.7	70.9	81.5	32.7	28.0	10.10
	1	47.8	54.2	72.6	81.5	33.7	32.3	11.66
	8	50.8	56.8	72.9	82.0	31.2	37.4	13.50

T_m^{on} , onset melting temperature; T_m^{pl} , peak position in low melting temperature range; T_m^{ph} , peak position in high melting temperature range; T_m^{f} , final melting temperature; $\Delta T_m = T_m^{\text{f}} - T_m^{\text{on}}$; ΔH_m , enthalpy of fusion; X_c , relative crystallinity.

55.8°C of EVA18 and 32.7°C of EVA28 because EVA14 has lower onset and higher final melting temperature, so it can be inferred that before aging EVA14 has wider crystals size distribution. In addition, the semi-crystalline EVA copolymer commonly has low crystallinity due to the disruptive effect of VAc comonomer. It can be observed from Table III

that the crystallinity of EVA14 and EVA18 are only from 27 to 23%; nevertheless, the crystallinity of EVA28 is about 10% which is no more than half of EVA14 or EVA18. As damp-heat aging time increases, the crystallinity values of the three copolymers are all enhanced with the content depending on the VAc content, similar with WAXD data.

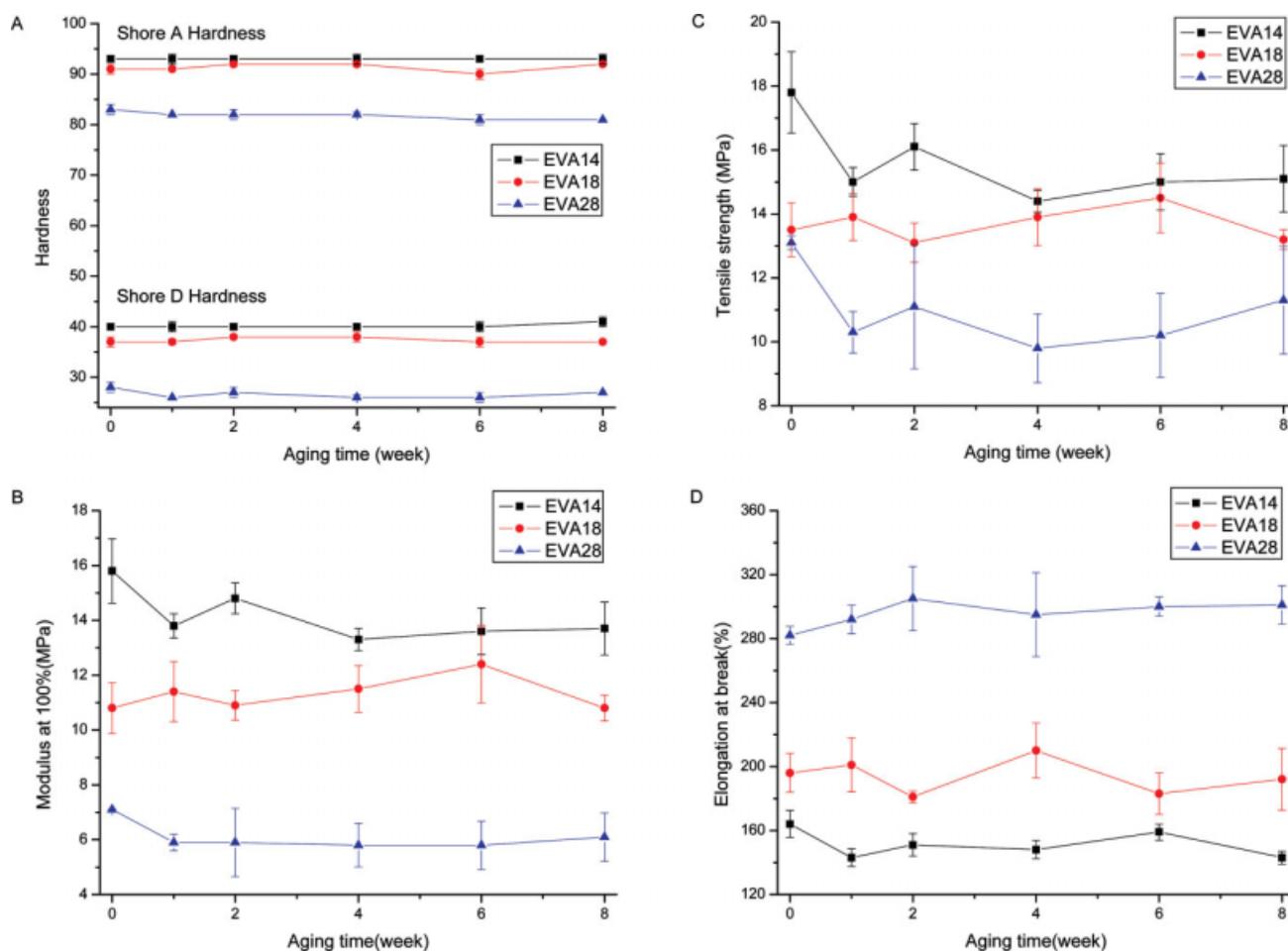


Figure 4 (A) Hardness; (B) Modulus at 100%; (C) Tensile strength; and (D) elongation at break changes before and after damp-heat aging for several weeks. [Color figure can be viewed in the online issue, which is available at www.interscience.wiley.com.]

Mechanical properties

To get a general study of the microscopic changes of structure and properties, macroscopic properties such as hardness, modulus, tensile strength and elongation at break were also investigated as follows.

Hardness

Hardness results of the three EVA copolymers with different damp-heat aging time are plotted in Figure 4(A). As can be seen from the graph, before aging both the Shore A and Shore D hardness go down with increasing VAc content. This is consistent with the fact that the surface hardness reduces with increase in VAc content.²⁸ It has been confirmed from Table III that the crystallinity which determines the hardness decreases with VAc content, so EVA28 has lower hardness than EVA14 or EVA18. Moreover, it is expected that the hardness of these EVA copolymers will increase after damp-heat aging, especially for EVA28, as crystallization analysis by DSC has proved that the aging resulted in the increase of crystallinity. However, Figure 4(A), obviously shows that there is no increase trace of the hardness at all. Therefore, it can be inferred that hardness is mainly correlated to first crystallization and it would not be changed despite the increase of secondary crystallization due to damp-heat aging. Another possible reason for the unchanged hardness is taken into account. Shore hardness was determined on overlapped samples of more than 5-cm thick whereas the samples for DSC analysis were merely 0.3-mm thick. So the increase of crystallinity was considered to occur only on the upper layer of the samples. That is why there are no changes in hardness but there are obvious changes in DSC curves.

Modulus at 100%

Modulus at 100% of the EVA copolymer is equal to the tensile stress at 100% elongation and is plotted versus the aging time in Figure 4(B). It is mainly determined by crystallinity of the polymer as is the case of hardness, so the decreases of modulus at 100% with increasing VAc content is observed from Figure 4(B). However, the increase of modulus at 100% is not observed like hardness and the unchanged results can also be attributed to the unchanged primary crystallization. It seems that the modulus of EVA14 and EVA28 has a slight decrease with aging time from the graph. However, the variation is not enough to be ascribed to the effect of the damp-heat aging and is mainly correlated to the deviation during sample preparations and tests.

Tensile strength and elongation at break

The tensile strength and elongation at break changes are displayed in Figure 4(C,D), respectively. As can be seen, the tensile strength and elongation at break depend much on the VAc content. EVA28 has smaller tensile strength and higher elongation at break than EVA14 or EVA18. Unlike the thermal aging of LDPE investigated by Bikiaris et al,³² both the tensile strength and elongation at break keep leveling off during whole aging process. The results indicate that the damp-heat aging has no quantitative or qualitative effect on the tensile properties of these EVA copolymers. It could be related to its saturated molecular structure which endows it good resistance to the damp-heat aging condition.

CONCLUSIONS

CI values derived from ATR-FTIR spectra first decrease and then increase during damp-heat aging process, which suggests the first loss then incorporation of O=C group. Observed by WAXD, no transformation of crystalline phase occurs, and crystal size changes differently for these EVA copolymers with different VAc contents. However, the narrowing trend of FWHM and increase of crystal sizes may be attributed to the melting and re-crystallization of secondary crystallization. DSC results confirm that primary crystallization has a close relationship with the VAc content and is independent of the damp-heat aging. In addition, the mechanical properties of the EVA copolymers show no obvious changes after damp-heat aging for even total 8 weeks.

References

1. Copuroglu, M.; Sen, M. *Polym Adv Technol* 2004, 15, 393.
2. Whelan, A.; Lee, K. S. *Developments in Rubber Technology-3 Thermoplastic Rubbers*; Applied Science Publishers: London, 1982.
3. Rodriguez-Vazquez, M.; Liauw, C. M.; Allen, N. S.; Edge, M.; Fontan, E. *Polym Degrad Stab* 2005, 91, 154.
4. Kamath, P. M.; Wakefield, R. W. *J Appl Polym Sci* 1965, 9, 3153.
5. Sultan, B. A.; Soervik, E. *J Appl Polym Sci* 1991, 43, 1737.
6. Sultan, B. A.; Soervik, E. *J Appl Polym Sci* 1991, 43, 1747.
7. Sultan, B. A.; Soervik, E. *J Appl Polym Sci* 1991, 43, 1761.
8. El-Din, N. M. S. *J Appl Polym Sci* 1993, 47, 911.
9. Allen, N. S.; Edge, M.; Rodriguez, M.; Liauw, C. M.; Fontan, E. *Polym Degrad Stab* 2000, 71, 1.
10. Tian, J.; Jiang, H.; Su, T.; Zhang, X.; Sun, Z. *Fenxi Ceshi Xuebao* 2003, 22, 100.
11. Marcilla, A.; Gomez, A.; Menargues, S. *J Anal Appl Pyrolysis*, 2005, 74, 224.
12. Marcilla, A.; Gomez-Siurana, A.; Menargues, S. *Thermochim Acta* 2005, 438, 155.
13. Czanderna, A. W.; Pern, F. J. *Sol Energy Mater Sol Cells* 1996, 43, 101.
14. Pern, F. J. *Sol Energy Mater Sol Cells* 1996, 587, 41.
15. Pern, F. J. *Angew Makromol Chem* 1997, 252, 195.

16. Klemchuk, P.; Ezrin, M.; Lavigne, G.; Holley, W.; Galica, J.; Agro, S. *Polym Degrad Stab* 1997, 55, 347.
17. Pern, F. J.; Glick, S. H. *Sol Energy Mater Sol Cells* 2000, 61, 153.
18. Parretta, A.; Bombace, M.; Graditi, G.; Schioppo, R. *Sol Energy Mater Sol Cells* 2005, 86, 349.
19. Mirabella, F. M. *J Polym Sci Polym Phys Ed* 1982, 20, 2309.
20. Liu, M.; Horrocks, R. A.; Hall, M. E. *Polym Degrad Stab* 1995, 49, 151.
21. Lacoste, J.; Carlsson, D. J. *J Polym Sci Part A: Polym Chem* 1992, 30, 493.
22. Suryanarayana, C.; Norton, M. G. *X-ray Diffraction: A Practical Approach*; Plenum Press: New York, 1998.
23. Brandrup, J.; Immergut, E. H.; Grulke, E. A. *Polymer Handbook*; Wiley-Interscience: New York, 1999.
24. Akpalu, Y.; Kielhorn, L.; Hsiao, B. S.; Stein, R. S.; Russell, T. P.; van Egmond, J.; Muthukumar, M. *Macromolecules* 1999, 32, 765.
25. Bassett, D. C. *Principles of Polymer Morphology*; Cambridge University Press: Cambridge, 1981.
26. Moly, K. A.; Radosch, H. J.; Androsh, R.; Bhagawan, S. S.; Thomas, S. *Eur Polym J* 2005, 41, 1410.
27. Russell, K. E.; Hunter, B. K.; Heyding, R. D. *Polymer* 1997, 38, 1409.
28. Henderson, A. M. *IEEE Electr Insul Mag* 1993, 9, 30.
29. Alizadeh, A.; Richardson, L.; Xu, J.; McCartney, S.; Marand, H.; Cheung, Y. W.; Chum, S. *Macromolecules* 1999, 32, 6221.
30. Feng, L.; Kamal, M. R. *Polym Eng Sci* 2005, 45, 1140.
31. Mavridis, H. *J Plast Film Sheet* 2002, 18, 259.
32. Bikiaris, D.; Prinos, J.; Panayiotou, C. *Polym Degrad Stab* 1997, 56, 1.